

Article

Modeling the Interplay between HDV and HBV in Chronic HDV/HBV Patients

Adequate Mhlanga ^{1,†}, Rami Zakh ^{2,3,†}, Alexander Churkin ³, Vladimir Reinharz ⁴, Jeffrey S. Glenn ⁵, Ohad Etzion ⁶, Scott J. Cotler ¹, Cihan Yurdaydin ^{7,*}, Danny Barash ^{2,*}  and Harel Dahari ^{1,*} 

¹ The Program for Experimental and Theoretical Modeling, Division of Hepatology, Department of Medicine, Stritch School of Medicine, Loyola University Chicago, Maywood, IL 84101, USA

² Department of Computer Science, Ben-Gurion University, Beer-Sheva 84105, Israel

³ Department of Software Engineering, Sami Shamoon College of Engineering, Beer-Sheva 84108, Israel

⁴ Department of Computer Science, Université du Québec à Montréal, Montréal, QC H3C 3P8, Canada

⁵ Division of Gastroenterology and Hepatology, Departments of Medicine, Microbiology & Immunology, Stanford School of Medicine, Stanford, CA 94305, USA

⁶ Department of Gastroenterology and Liver Diseases, Soroka University Medical Center, Beer-Sheva 84101, Israel

⁷ Department of Gastroenterology and Hepatology, Koç University Medical School, Istanbul 34450, Turkey

* Correspondence: cyurdaydin@ku.edu.tr (C.Y.); dbarash@cs.bgu.ac.il (D.B.); hdahari@luc.edu (H.D.)

† These authors contributed equally to this work.

Abstract: Hepatitis D virus is an infectious subviral agent that can only propagate in people infected with hepatitis B virus. In this study, we modified and further developed a recent model for early hepatitis D virus and hepatitis B virus kinetics to better reproduce hepatitis D virus and hepatitis B virus kinetics measured in infected patients during anti-hepatitis D virus treatment. The analytical solutions were provided to highlight the new features of the modified model. The improved model offered significantly better prospects for modeling hepatitis D virus and hepatitis B virus interactions.

Keywords: hepatitis delta virus; hepatitis B virus; anti-HDV treatment; analytical solution

MSC: 92-10



Citation: Mhlanga, A.; Zakh, R.; Churkin, A.; Reinharz, V.; Glenn, J.S.; Etzion, O.; Cotler, S.J.; Yurdaydin, C.; Barash, D.; Dahari, H. Modeling the Interplay between HDV and HBV in Chronic HDV/HBV Patients. *Mathematics* **2022**, *10*, 3917. <https://doi.org/10.3390/math10203917>

Academic Editor: Carla M.A. Pinto

Received: 7 September 2022

Accepted: 19 October 2022

Published: 21 October 2022

Publisher's Note: MDPI stays neutral with regard to jurisdictional claims in published maps and institutional affiliations.



Copyright: © 2022 by the authors. Licensee MDPI, Basel, Switzerland. This article is an open access article distributed under the terms and conditions of the Creative Commons Attribution (CC BY) license (<https://creativecommons.org/licenses/by/4.0/>).

1. Introduction

Chronic hepatitis D virus (HDV) is a serious clinical concern with an estimated prevalence of ~10–20 million persons worldwide [1,2]. It was first described by Rizzetto and colleagues in the mid-1970s in patients with chronic hepatitis B virus (HBV) infection [3]. It was found that HDV requires the presence of HBV infection to assemble infectious HDV progeny virions [4]. In addition, HDV and HBV need the same proteins to enter hepatocytes [5]. There is no therapy approved for HDV by the US Food and Drug Administration [6]. Pegylated interferon- α treatment [7], which is endorsed by expert guidelines [8,9] with suboptimal outcomes, affects both HDV and HBV, which precludes modeling the interplay between the HBV and HDV [10].

Because HBV and HDV replicate in the same cells and influence each other and the host, we recently developed the first mathematical model to reproduce HDV and HBV kinetics in two patients receiving the prenylation inhibitor Lonafarnib (termed here anti-HDV) treatment in the absence of an anti-HBV therapy [11]. In the current study, we showed that the published model in [11] failed to explain the additional patients' kinetic data reported in the LOWR HDV-1 (Lonafarnib with and without Ritonavir in HDV-1) study by Yurdaydin et al. [12] and suggested modifications to the model along with its analytical solutions. We provided the analytical solution of the improved model for both HDV and HBV using hypergeometric functions for HBV [13].

2. Background

We recently developed a model [11], that accounts for both HDV and HBV dynamics after the onset of anti-HDV treatment using the following differential equations:

$$\frac{dD}{dt} = (1 - \epsilon)p_1 I_0 e^{-gt} - cD(t) \tag{1}$$

$$\frac{dB}{dt} = p_2 I_0 n^{-4} \left(\frac{D_0}{D(t)} \right)^n - cB(t) \tag{2}$$

where D and B represent the HDV viral load and HBV viral load in blood, respectively. Parameters p_1 and p_2 represent the production rate constant of HDV and HBV from infected cell number, I_0 . We assumed that the clearance rate constant, c , is the same for HDV and HBV and that it is within the range of the HDV clearance rate estimated in [14,15]. Parameter ϵ represents the efficacy of the treatment for HDV, with $0 < \epsilon < 1$, and g is the assumed additional treatment inhibitory effect in blocking HDV production as previously conducted under antiviral treatment for HBV [16,17]. Parameter n governs the HBV production rate increase under anti-HDV treatment.

Before treatment, HBV and HDV levels are in equilibrium with the production rate of HDV given by

$$p_1 = (cD_0)/I_0 \tag{3}$$

and that of HBV represented by

$$p_2 = (cB_0)/I_0 \tag{4}$$

where D_0 and B_0 are the HDV and HBV levels at the onset of treatment, respectively. The number of the infected cells, I_0 , was kept constant under treatment and prior to treatment onset, where $\epsilon = g = 0$, and $n = 1$.

The original model Equations (1) and (2) simulated well the digitized serum HBV DNA and HDV kinetic data in two patients that were provided in Figure 5 in [12]. The two digitized patients displayed a moderate decrease in the second phase of HDV decline (i.e., low parameter g values) during anti-HDV treatment along with a sharp increase in HBV levels that could be reproduced by the model, as recently shown in Figures 3 and 4 in [11]. However, in the current study, we reported that the original model Equations (1) and (2) failed to explain additional patients who had a faster second phase decline in HDV (i.e., higher parameter g values) concomitantly with a moderate (or extremely slow) increase in HBV levels (Figure 1).

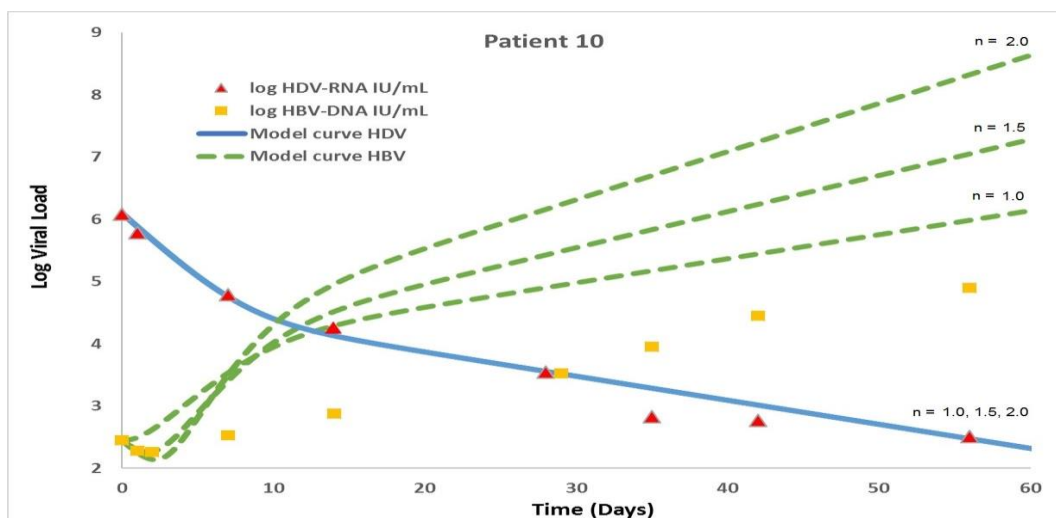


Figure 1. The model Equations (1) and (2) failed to reproduce HBV kinetics in additional patients reported in Yurdaydin et al. [5]. Model parameter values were $D_0 = 1.2 \times 10^6$, $B_0 = 282$, $c = 0.51$, $g = 0.089$, $\epsilon = 0.97$.

3. Modified Model

To address the inability of the model Equations (1) and (2) to reproduce HDV and HBV kinetics in some patients (Figure 1), we modified Equation (2) by replacing the term $n^{-4}(D_0/D(t))^n$ with a $(1 + (\kappa/D(t))^n)$ as follows and in Figure 2.

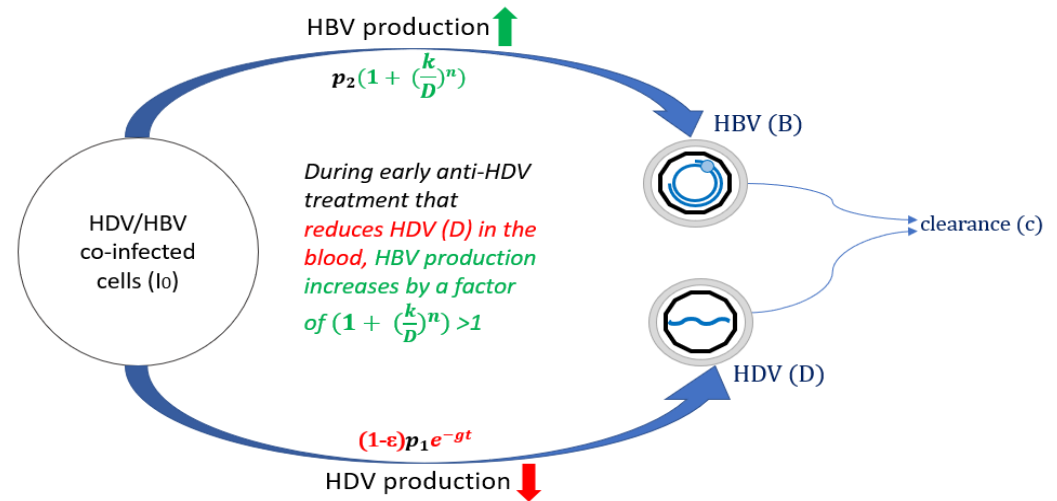


Figure 2. Schematic diagram for the modified model, Equations (1) and (5).

Obtaining

$$\frac{dB}{dt} = p_2 I_0 \left(1 + \left(\frac{\kappa}{D(t)}\right)^n\right) - cB \tag{5}$$

where κ represents the threshold HDV level in blood that triggers an increase in HBV production, and κ is unique to each patient. As an example, in a patient with pre-treatment $\kappa/D_0 \sim 0$, as $D(t)$ decreased under treatment, because $D_0 > \kappa$, the production of HBV increased, e.g., at time t_1 after the initiation of treatment. When $D(t_1) = \kappa$, the pre-treatment HBV production p_2 doubled (Figure 3). The time t_1 at which p_2 double depends on the pre-treatment ratio κ/D_0 as shown in Figure 3.

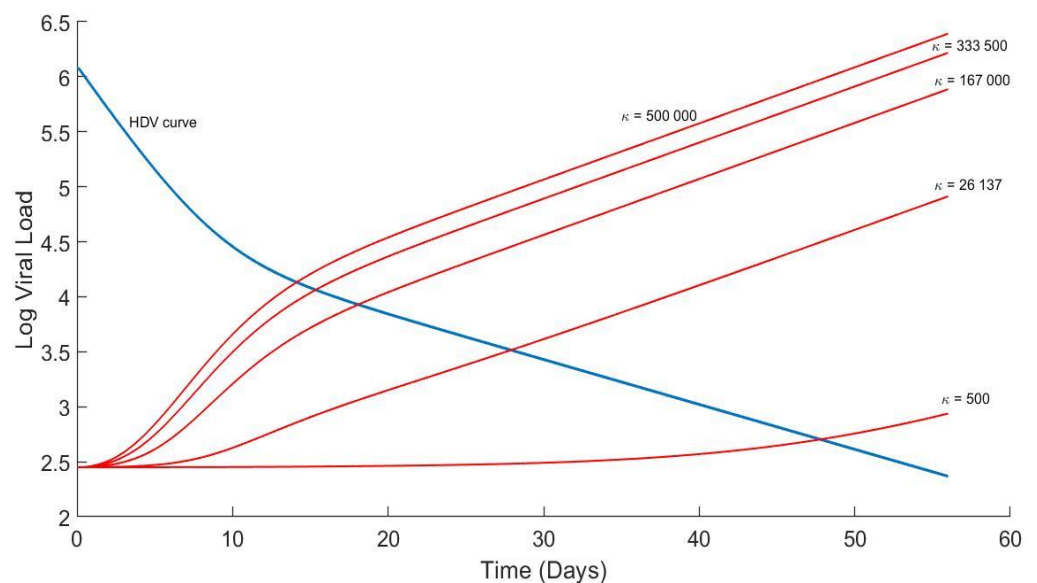


Figure 3. One-way sensitivity analysis on the impact of parameter κ on predicted HBV kinetics, B, (red curves) under anti-HDV treatment. Model parameters were set to $D_0 = 1,202,260$, $B_0 = 282$, $c = 0.47$, $n = 1.25$, $g = 0.094$, $\tau = 0.1$, and $\varepsilon = 0.97$. HDV predicted kinetics, D (blue curve) was not affected by different κ values.

Before treatment, the HBV and HDV are in equilibrium, with the production rate of HDV given by p_1 in Equation (3), and p_2 for HBV in Equation (4) is replaced by

$$p_2 = \frac{cB_0}{I_0 \left(1 + \left(\frac{\kappa}{D_0} \right)^n \right)} \tag{6}$$

The number of the infected cells, I_0 , was kept constant under treatment and prior to treatment onset, where $\varepsilon = g = 0$ as assumed in the original model. Furthermore, we assumed that HDV decay begins at time τ (days), corresponding to the delay observed in the data and possibly reflecting Lonafarnib pharmacokinetics.

A one-way sensitivity analysis of our proposed model was carried out to investigate its robustness. The sensitivity analysis was carried out on the fittings for patient 10 as shown in Figures A1–A5, which are provided in Appendix A. We introduced some noise into our model by varying five parameters (g , c , n , ε , and κ) with a variation of $+/- 10\%$ around our baseline values. It is worth stating that the variation range of ε was a bit lower than $+/- 10\%$, since it was already closer to its upper bound, i.e., 1. We can clearly see that varying c , n , and k had no impact on the HDV dynamics, while varying g and ε had a small impact. Additionally, it can be noted that varying of all the five parameters had no major effect on the HBV dynamics.

4. Results

4.1. The Modified Model Simulates the Measured Data

Using the Berkely Madonna software (berkeley-madonna.myshopify.com (accessed on 1 August 2022)) with the standard Runge–Kutta scheme of the fourth order, we reproduced the data well, as shown for four representative patients (Figure 4).

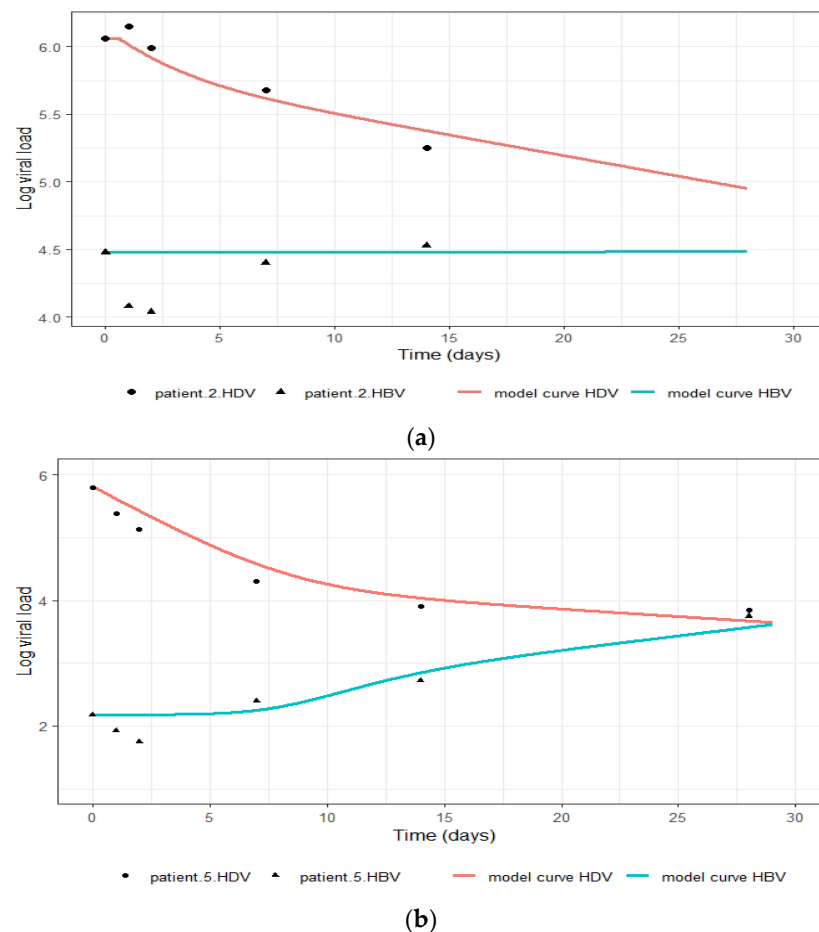


Figure 4. Cont.

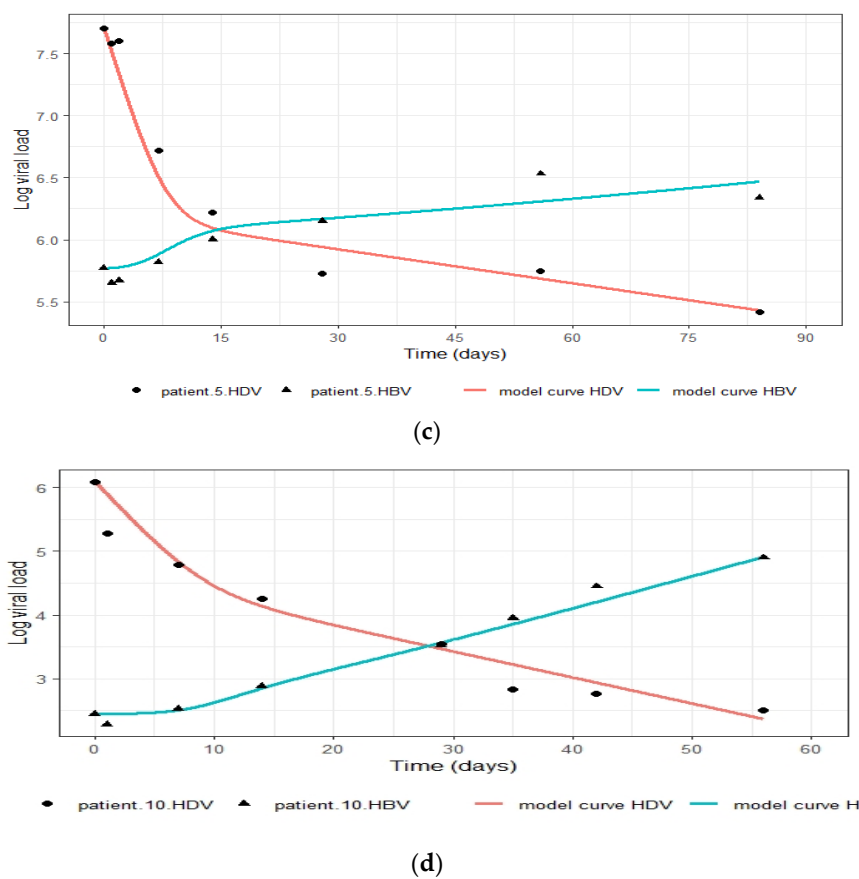


Figure 4. Model agreement with measured HDV RNA (circles) and HBV DNA (triangles) kinetics in four representative patients. Model parameters were (a) $B_0 = 30,200$, $D_0 = 1.14815 \times 10^6$, $\epsilon = 0.53$, $g = 0.077$, $n = 1.8$, and $\kappa = 9799$, (b) $B_0 = 151$, $D_0 = 6.30957 \times 10^5$, $\epsilon = 0.97$, $g = 0.054$, $n = 2$, and $\kappa = 25,503$, (c) $B_0 = 5.88844 \times 10^5$, $D_0 = 5.01187 \times 10^7$, $\epsilon = 0.97$, $g = 0.020$, $n = 1.1$, and $\kappa = 1.23198 \times 10^6$, and (d) $B_0 = 282$, $D_0 = 1.20226 \times 10^6$, $\epsilon = 0.97$, $g = 0.094$, $n = 1.25$, and $\kappa = 26,137$. The other model parameters c and τ were fixed to 0.47 and 0.1, respectively, except for Patient 2 with $\tau = 0.6$, as depicted in Figure 4a.

4.2. Analytic Solutions

This subsection sought to determine the analytical solutions for $D(t)$ and $B(t)$. The analytical solution of $D(t)$ was already solved in [11] and is provided herein again for convenience.

4.3. Analytic Solutions for HDV

We can derive the analytical solution of $D(t)$ as follows:
From Equation (1), we have that

$$\frac{dD}{dt} + cD = (1 - \epsilon)p_1e^{-gt}I_0. \tag{7}$$

We then determined the integrating factor as, e^{ct} , and by multiplying both sides of Equation (7) by the integrating factor, we have

$$\frac{d}{dt}(De^{ct}) = (1 - \epsilon)p_1e^{-gt}I_0 e^{ct}. \tag{8}$$

By integrating both sides of the Equation (8), it follows that

$$(De^{ct}) = Me^{-gt} e^{ct} + K, \tag{9}$$

with $M = \frac{(1-\epsilon)p_1e^{-gt}I_0D}{c-g}$, which then simplifies to

$$D = Me^{-gt} e^{ct} + Ke^{-ct}. \tag{10}$$

At time $t = 0$, we have $D = D_0$, and evaluating Equation (10) we now have

$$K = D_0 - M.$$

Thus, the exact solution for D is given by

$$D(t) = Me^{-gt} + (D_0 - M)e^{-ct} \tag{11}$$

4.4. Analytical Solution for HBV and Plots

Using Wolfram Mathematica version 13.0.1.0, we managed to determine the analytical solution for $B(t)$. Thus, the analytical solution of HBV (Equation (5)) is given by

$$\begin{aligned}
 &b[t] \\
 &\rightarrow e^{-ct}(B_0 \\
 &+ \int_0^t \frac{B_0 \cdot c \cdot e^{cx} \left(1 + \left(-\frac{e^{cx}(c-g)k}{D_0 \cdot (-c \cdot e^{(c-g)x} + c \cdot e^{(-1+e^{(c-g)x})+g})} \right)^n \right)}{1 + \left(\frac{k}{D_0} \right)^n} dx)
 \end{aligned} \tag{12}$$

Using the Berkeley Madonna simulation for the newly simulated Patient 10, we found its best-fit parameters:

$$n = 1.25, \epsilon = 0.97, g = 0.094, k = 26137 \text{ and } c = 0.47$$

With the above, the HBV analytical solution becomes

$$\begin{aligned}
 &b[t] \\
 &\rightarrow 279.66 + 1.28e^{-0.47t} \\
 &+ 35.70 \left(\frac{1}{1157175.25e^{-0.47t} + 45084.75e^{-0.094t}} \right)^{1.25} (1157175.25 \\
 &+ 45084.75e^{0.376t})^1 \cdot \text{Hypergeometric2F1} \left[1, 2.5625, 3.8125, -0.039e^{0.376t} \right]
 \end{aligned} \tag{13}$$

where Hypergeometric2F1 is the Gaussian hypergeometric function ${}_2F_1(\alpha, \beta; \gamma; z)$, where α, β , and γ are the function parameters and z is the variable of the Gaussian hypergeometric function.

In Figure 5, we show the simulations of the HDV and HBV plots for Patient 10.

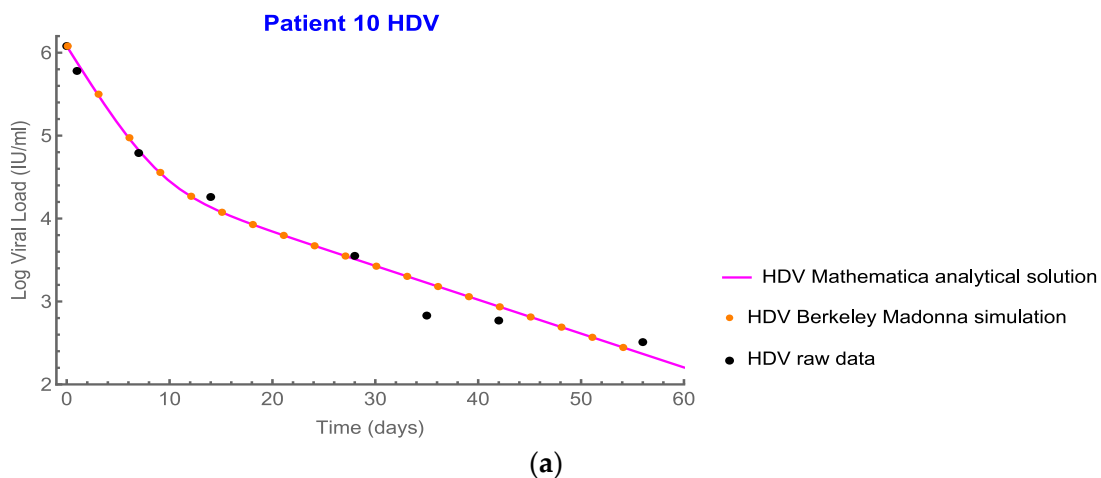


Figure 5. Cont.

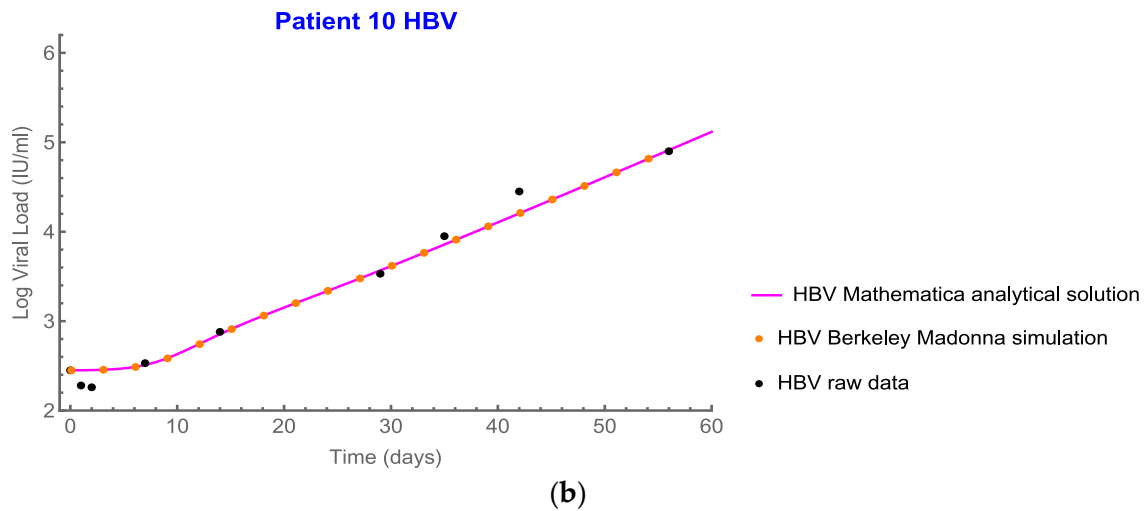


Figure 5. (a) shows the HBV Mathematica analytical solution (i.e., Equation (13) herein), HBV Berkeley Madonna fit for Patient 10, which was a result of fitting the modified model Equations (1) and (5) with measured data using Berkeley Madonna. (b) follows a similar approach as conducted in 5a but for HDV using D.

Using the Berkeley Madonna simulation for Patient 2, we found its best-fit parameters:

$$n = 1.80, \varepsilon = 0.53, g = 0.070, k = 9799 \text{ and the constant } c = 0.47$$

With the above, the HBV analytical solution becomes

$$\begin{aligned}
 &b[t] \\
 &\rightarrow 30194.30 + 2.98e^{-0.47t} \\
 &+ 320523.47e^{-1.66 \times 10^{-16}t} \left(\frac{1}{514084.16e^{-0.47t} + 634065.8375e^{-0.07t}} \right)^{1.8} (514084.16 \\
 &+ 634065.84e^{0.4t})^1 \cdot \text{Hypergeometric2F1} \left[1, 2.49, 4.29, -1.23e^{0.4t} \right]
 \end{aligned} \tag{14}$$

In Figure 6, we show the simulations of HDV and HBV plots for Patient 2.

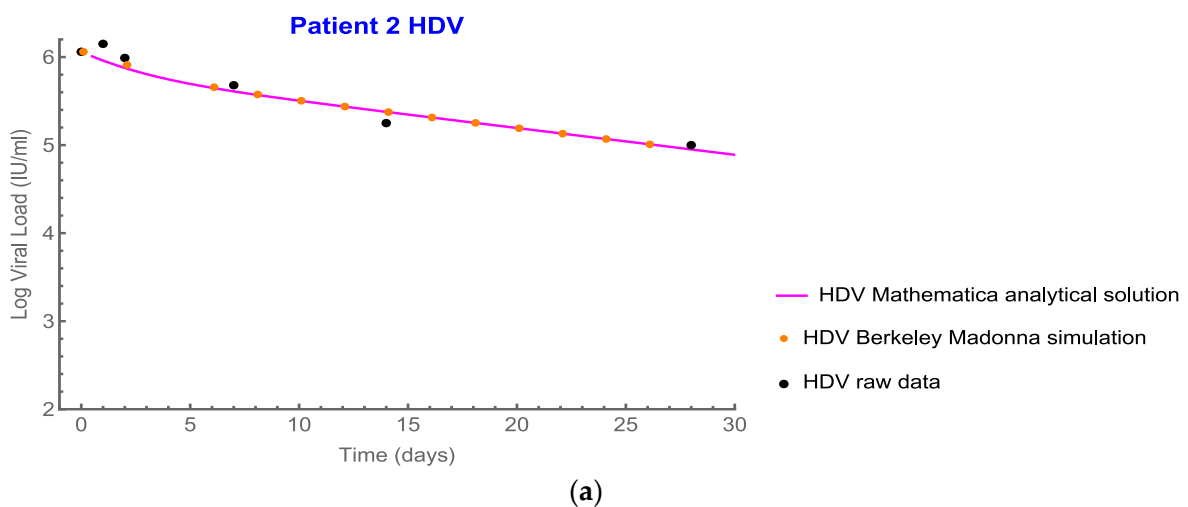


Figure 6. Cont.

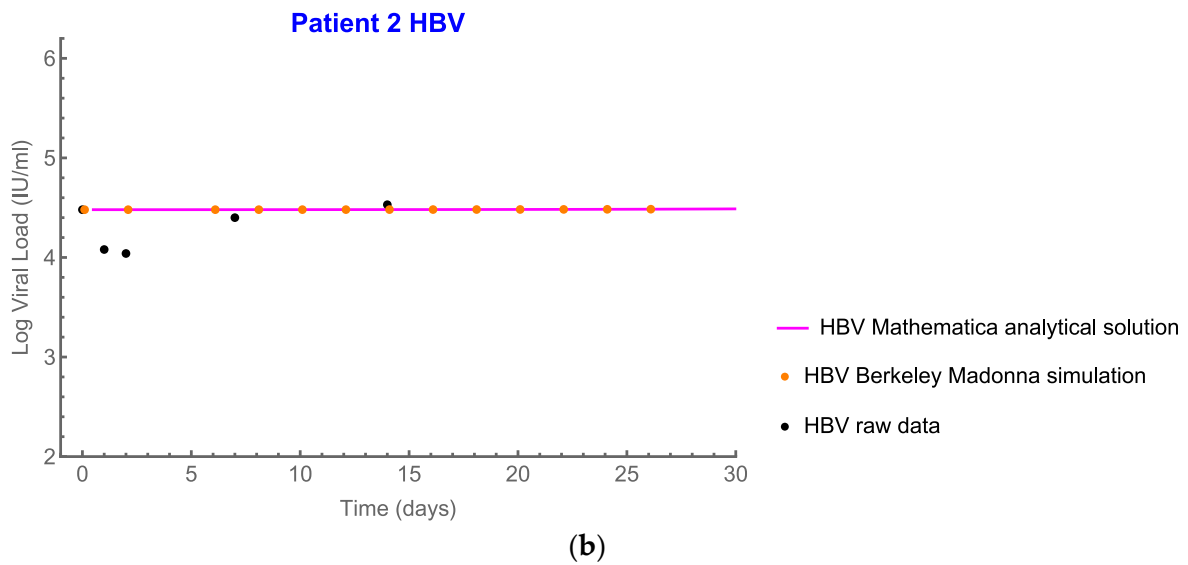


Figure 6. (a) shows the HBV Mathematica analytical solution (i.e., Equation (14) herein), HBV Berkeley Madonna fit for Patient 2, which was a result of fitting the modified model with measured data using Berkeley Madonna as reported in [4] and the HBV raw data. (b) follows a similar approach as conducted in 6a but for HDV using D.

Using the Madonna simulation for Patient 4, we found its best-fit parameters:

$$n = 2.00, \epsilon = 0.97, g = 0.054, k = 25503 \text{ and the constant } c = 0.47$$

With the above, the HBV analytical solution becomes

$$\begin{aligned}
 b[t] &\rightarrow 150.75 + 0.16e^{-0.47t} \\
 &+ 53617.29 \left(\frac{1}{609571.20e^{-0.47t} + 21385.80e^{-0.054t}} \right)^2 \cdot (609571.20 \\
 &+ 21385.80e^{0.416t})^1 \cdot \text{Hypergeometric2F1} \left[1, 2.39, 4.39, -0.035e^{0.416t} \right]
 \end{aligned} \tag{15}$$

In Figure 7, we show the simulations of HDV and HBV plots for Patient 4.

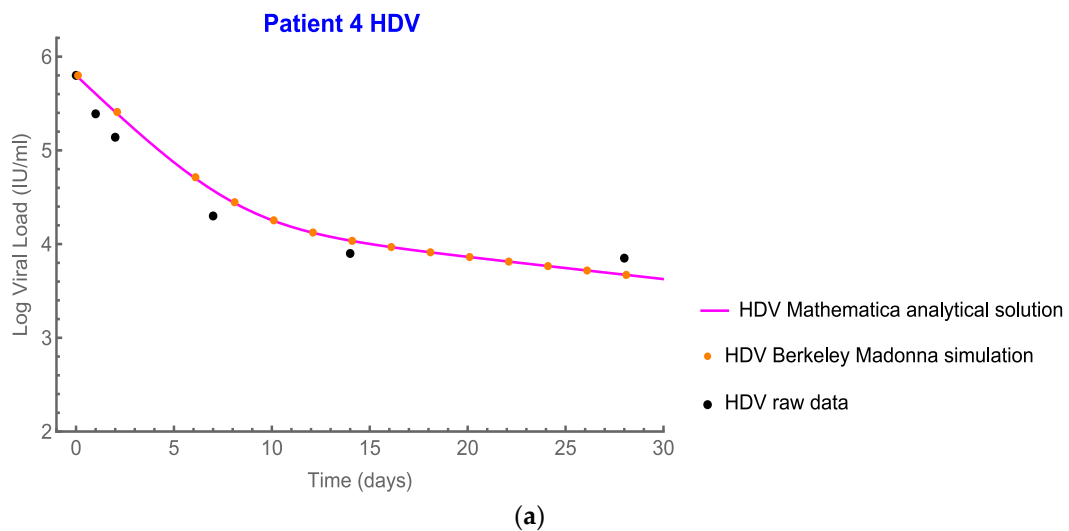


Figure 7. Cont.

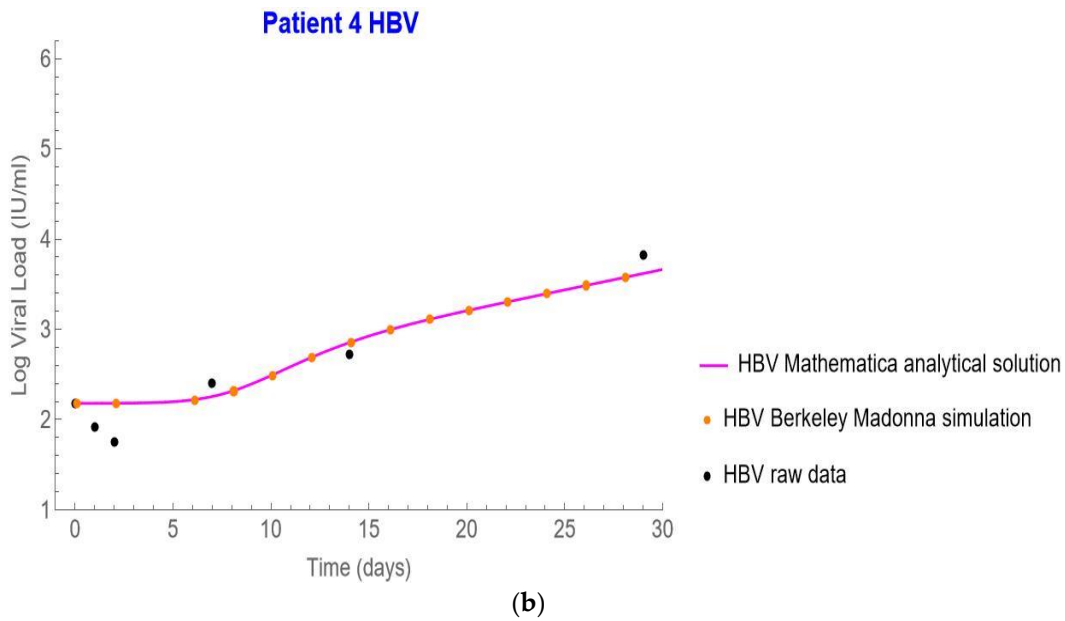


Figure 7. (a) shows the HBV Mathematica analytical solution (i.e., Equation (15) herein), HBV Berkeley Madonna fit for Patient 4, which is a result of fitting the modified model with measured data using Berkeley Madonna 7. (b) follows a similar approach as conducted in 7a but for HDV using D.

Using the Madonna simulation for the newly simulated Patient 5, we found its best-fit parameters:

$$n = 0.81, \varepsilon = 0.97, g = 0.021, k = 1716544 \text{ and the constant } c = 0.47$$

With the above, the HBV analytical solution becomes

$$\begin{aligned}
 b[t] &\rightarrow 552892.94 + 15911.46e^{-0.47t} \\
 &+ 706.14 \left(\frac{1}{4.85 \times 10^7 e^{-0.47t} + 1573883.45 e^{-0.021t}} \right)^{0.81} (4.85 \times 10^7 \\
 &+ 1573883.45 e^{0.449t})^1 \text{Hypergeometric2F1} \left[1, 2.08, 2.89, -0.032e^{0.449t} \right]
 \end{aligned} \tag{16}$$

In Figure 8, we show the simulations of HDV and HBV plots for Patient 5.

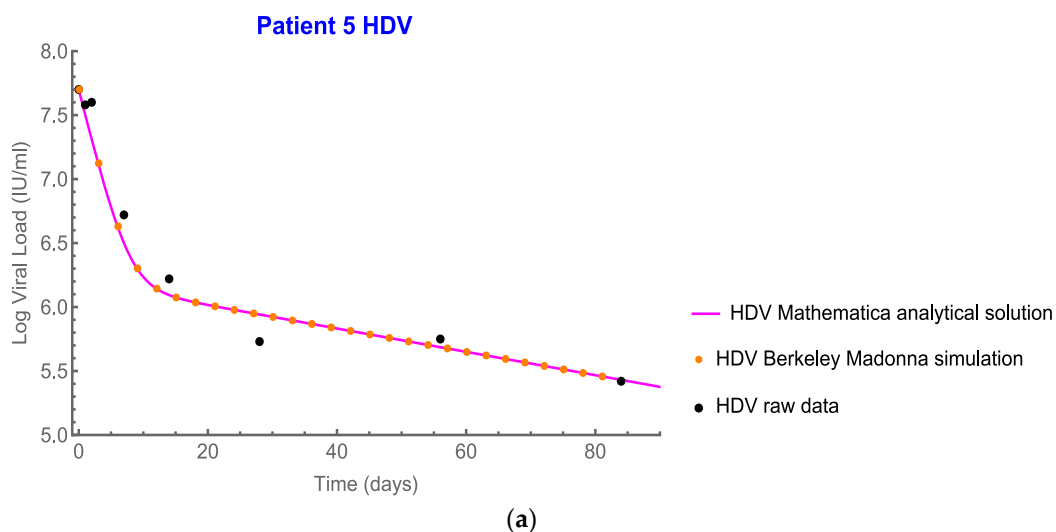


Figure 8. Cont.

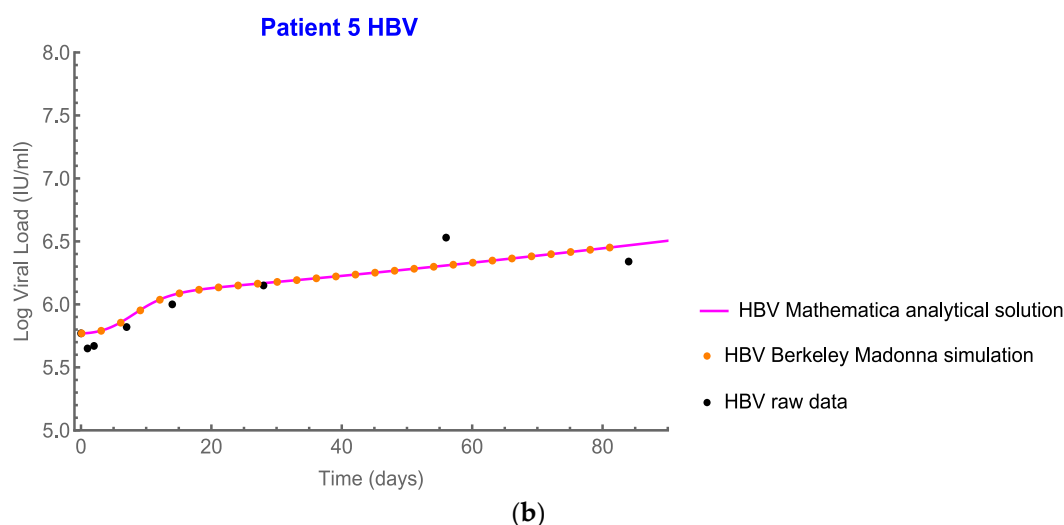


Figure 8. (a) shows the HBV Mathematica analytical solution (i.e., Equation (16) herein), HBV Berkeley Madonna fit for patient 5, which was a result of fitting the modified model with measured data using Berkeley Madonna 8. (b) follows a similar approach as conducted in 8a but for HDV using D.

5. Discussion and Conclusions

In this study, we provided additional insights into the interplay between HDV and HBV during anti-HDV treatment by suggesting a modification to our recently published mathematical model [4]. The modification was achieved by replacing the term $n^{-4}(D_0/D(t))^n$ in Equation (2) with a new term $(1+(\kappa/D))^n$ as shown in Equation (5). The term $(1+(\kappa/D))^n$ allowed starting with a pre-treatment HBV production rate, which could increase as a result of HDV decline by the several suggested mechanisms that were reviewed in [18]. The value of κ , which was unique for each patient (Figure 4), could represent, in part, the interplay between HDV and HBV.

The modified model could explain HDV decline with different HBV kinetic changes: (i) no change (Figure 4a), (ii) a delay followed by an increase (Figure 4b,d), and (iii) a fast increase followed by a slower increase (Figure 4c). In addition, we provided the analytical solution of the HBV modified model using hypergeometric functions [6].

In future work, our modified model could be examined in a much larger number of patients and anti-HDV combination therapies. The modified model could also be extended to account for additional biological features, e.g., immune response, molecular interactions, and/or susceptible and infected cell dynamics. In addition, previously reported HDV/HBV mathematical models [19–21] could be extended to account for the unique HDV and HBV dynamics proposed in this study. As such, the modified model is a better starting point for developing more comprehensive HDV/HBV models for understanding the interactions between HBV and HDV that, in turn, may help to design therapeutic strategies to fight HDV.

Author Contributions: Conceptualization, C.Y., D.B. and H.D.; methodology, A.M., R.Z., A.C., V.R., D.B. and H.D.; investigation, A.M., R.Z., A.C., V.R., J.S.G., C.Y., D.B. and H.D.; writing—original draft preparation, A.M., R.Z., A.C., V.R., D.B. and H.D.; writing—review and editing, S.J.C., O.E., C.Y. and J.S.G.; supervision, A.C., D.B. and H.D.; funding acquisition, R.Z., O.E., C.Y., D.B. and H.D. All authors have read and agreed to the published version of the manuscript.

Funding: This research was partly funded by the NIH grants R01AI144112 and R01AI146917.

Institutional Review Board Statement: Not applicable.

Data Availability Statement: All data used during this study will be provided upon request to the authors.

Acknowledgments: R.Z., O.E., H.D. and D.B. would like to thank SimReC—The research center for simulation in healthcare at Ben-Gurion University, and the Lynne and William Frankel Center for Computer Science at Ben-Gurion University.

Conflicts of Interest: Yurdaydin and Etzion are on the speakers’ bureau and received grants from Eiger. Glenn is the founder and a director of, holds intellectual property rights with, and owns stock and royalty rights from Eiger. The other authors declare no conflict of interest.

Appendix A

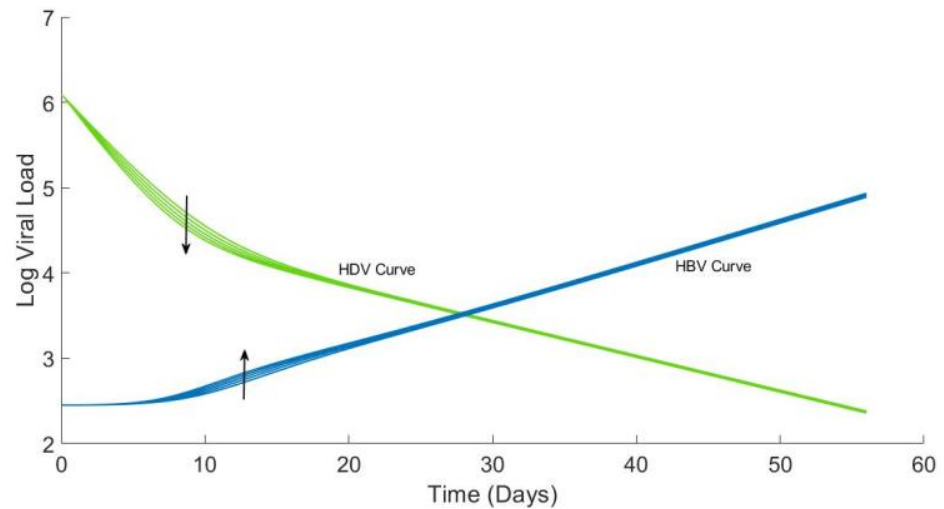


Figure A1. One-way sensitivity analysis on the impact of parameter c on predicted HBV/HDV kinetics under anti-HDV treatment. Model parameters were set to $D_0 = 1,202,260$, $B_0 = 282$, $\kappa = 26,137$, $n = 1.25$, $g = 0.094$, $\tau = 0.1$, and $\varepsilon = 0.97$, with c being set at $c = (0.423, 0.4465, 0.47, 0.4935, 0.517)$. The arrows depict the direction of increase of the parameter c .

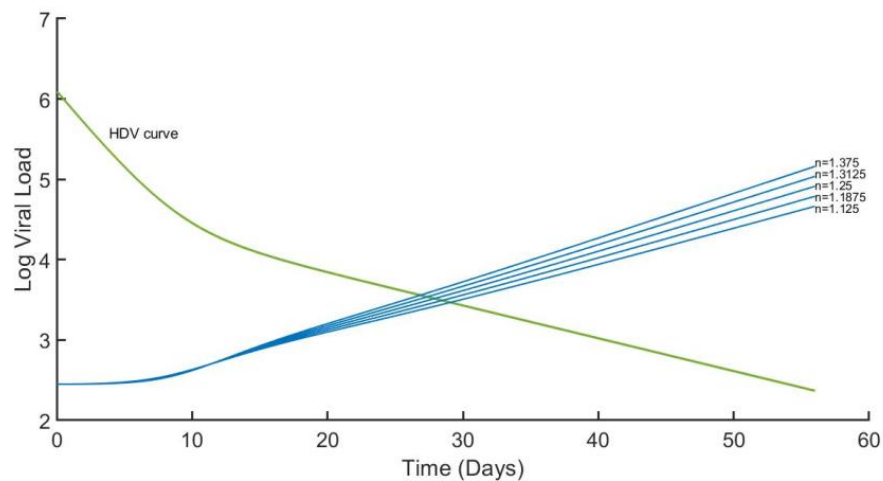


Figure A2. One-way sensitivity analysis on the impact of parameter n on predicted HBV/HDV kinetics under anti-HDV treatment. Model parameters were set to $D_0 = 1,202,260$, $B_0 = 282$, $\kappa = 26,137$, $c = 0.47$, $g = 0.094$, $\tau = 0.1$, and $\varepsilon = 0.97$, with n being set at $n = (1.125, 1.1875, 1.25, 1.3125, 1.375)$. HDV predicted kinetics were not affected by different n values.

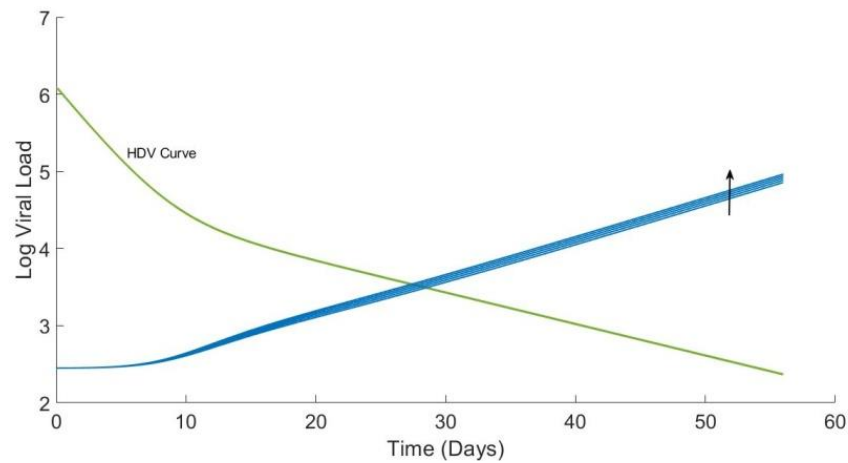


Figure A3. One-way sensitivity analysis on the impact of parameter κ on predicted HBV/HDV kinetics under anti-HDV treatment. Model parameters were set to $D_0 = 1,202,260$, $B_0 = 282$, $n = 1.25$, $c = 0.47$, $g = 0.094$, $\tau = 0.1$, and $\varepsilon = 0.97$, with κ being set at $\kappa = (23,523, 24,830, 26,137, 27,444, 28,751)$. The arrows depict the direction of increase of the parameter κ . HDV predicted kinetics were not affected by different n values.

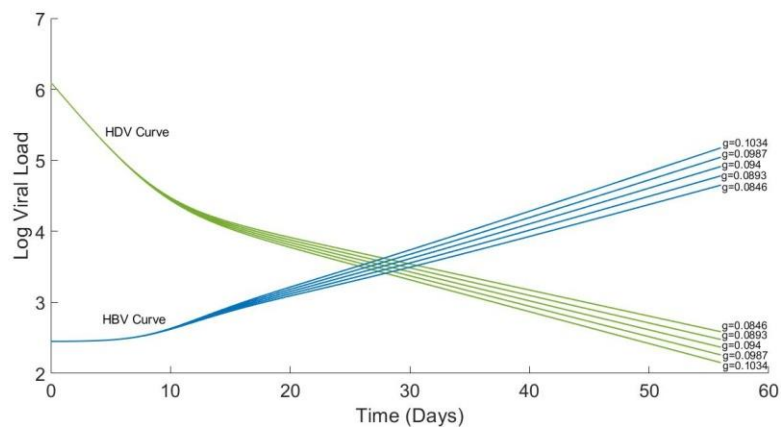


Figure A4. One-way sensitivity analysis on the impact of parameter g on predicted HBV/HDV kinetics under anti-HDV treatment. Model parameters were set to $D_0 = 1,202,260$, $B_0 = 282$, $\kappa = 26,137$, $c = 0.47$, $n = 1.25$, $\tau = 0.1$, and $\varepsilon = 0.97$, with g being set at $g = (0.0846, 0.0893, 0.094, 0.0987, 0.1034)$.

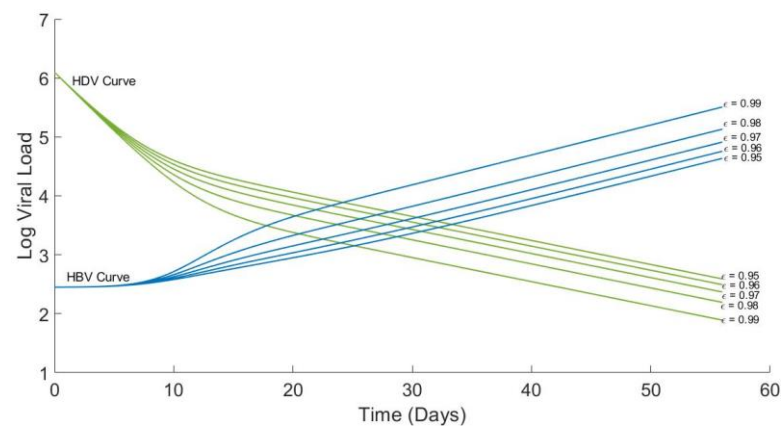


Figure A5. One-way sensitivity analysis on the impact of parameter ε on predicted HBV/HDV kinetics under anti-HDV treatment. Model parameters were set to $D_0 = 1,202,260$, $B_0 = 282$, $\kappa = 26,137$, $c = 0.47$, $n = 1.25$, $\tau = 0.1$, and $g = 0.094$, with ε being set at $\varepsilon = (0.95, 0.96, 0.97, 0.98, 0.99)$.

References

1. Stockdale, A.J.; Kreuels, B.; Henrion, M.Y.R.; Giorgi, E.; Kyomuhangi, I.; de Martel, C.; Hutin, Y.; Geretti, A.M. The global prevalence of hepatitis D virus infection: Systematic review and meta-analysis. *J. Hepatol.* **2020**, *73*, 523–532. [[CrossRef](#)] [[PubMed](#)]
2. Miao, Z.; Zhang, S.; Ou, X.; Li, S.; Ma, Z.; Wang, W.; Peppelenbosch, M.P.; Liu, J.; Pan, Q. Estimating the Global Prevalence, Disease Progression, and Clinical Outcome of Hepatitis Delta Virus Infection. *J. Infect. Dis.* **2020**, *221*, 1677–1687. [[CrossRef](#)] [[PubMed](#)]
3. Rizzetto, M.; Canese, M.G.; Arico, S.; Crivelli, O.; Trepo, C.; Bonino, F.; Verme, G. Immunofluorescence detection of new antigen-antibody system (delta/anti-delta) associated to hepatitis B virus in liver and in serum of HBsAg carriers. *Gut* **1977**, *18*, 997–1003. [[CrossRef](#)] [[PubMed](#)]
4. Koh, C.; Heller, T.; Glenn, J.S. Pathogenesis of and New Therapies for Hepatitis D. *Gastroenterology* **2019**, *156*, 461–476.e1. [[CrossRef](#)] [[PubMed](#)]
5. Engelke, M.; Mills, K.; Seitz, S.; Simon, P.; Gripon, P.; Schnolzer, M.; Urban, S. Characterization of a hepatitis B and hepatitis delta virus receptor binding site. *Hepatology* **2006**, *43*, 750–760. [[CrossRef](#)] [[PubMed](#)]
6. Yardeni, D.; Heller, T.; Koh, C. Chronic hepatitis D—What is changing? *J. Viral Hepat.* **2022**, *29*, 240–251. [[CrossRef](#)] [[PubMed](#)]
7. Heller, T.; Rotman, Y.; Koh, C.; Clark, S.; Haynes-Williams, V.; Chang, R.; McBurney, R.; Schmid, P.; Albrecht, J.; Kleiner, D.E.; et al. Long-term therapy of chronic delta hepatitis with peginterferon alfa. *Aliment. Pharmacol. Ther.* **2014**, *40*, 93–104. [[CrossRef](#)] [[PubMed](#)]
8. Terrault, N.A.; Lok, A.S.F.; McMahon, B.J.; Chang, K.M.; Hwang, J.P.; Jonas, M.M.; Brown, R.S., Jr.; Bzowej, N.H.; Wong, J.B. Update on prevention, diagnosis, and treatment of chronic hepatitis B: AASLD 2018 hepatitis B guidance. *Hepatology* **2018**, *67*, 1560–1599. [[CrossRef](#)] [[PubMed](#)]
9. European Association for the Study of the Liver. Electronic address eee, European Association for the Study of the L. EASL 2017 Clinical Practice Guidelines on the management of hepatitis B virus infection. *J. Hepatol.* **2017**, *67*, 370–398. [[CrossRef](#)] [[PubMed](#)]
10. Guedj, J.; Rotman, Y.; Cotler, S.J.; Koh, C.; Schmid, P.; Albrecht, J.; Haynes-Williams, V.; Liang, T.J.; Hoofnagle, J.H.; Heller, T.; et al. Understanding early serum hepatitis D virus and hepatitis B surface antigen kinetics during pegylated interferon-alpha therapy via mathematical modeling. *Hepatology* **2014**, *60*, 1902–1910. [[CrossRef](#)]
11. Zakh, R.; Churkin, A.; Bietsch, W.; Lachiany, M.; Cotler, S.J.; Ploss, A.; Dahari, H.; Barash, D. A Mathematical Model for early HBV and -HDV Kinetics during Anti-HDV Treatment. *Mathematics* **2021**, *9*, 3323. [[CrossRef](#)] [[PubMed](#)]
12. Yurdaydin, C.; Keskin, O.; Kalkan, C.; Karakaya, F.; Caliskan, A.; Karatayli, E.; Karatayli, S.; Bozdayi, A.M.; Koh, C.; Heller, T.; et al. Optimizing lonafarnib treatment for the management of chronic delta hepatitis: The LOWR HDV-1 study. *Hepatology* **2018**, *67*, 1224–1236. [[CrossRef](#)] [[PubMed](#)]
13. Olde, D.; Adri, B. *NIST Handbook of Mathematical Functions*; Cambridge University Press: Cambridge, UK, 2010.
14. Shekhtman, L.; Cotler, S.J.; Hershkovich, L.; Uprichard, S.L.; Bazinet, M.; Pantea, V.; Ceboatarescu, V.; Cojuhari, L.; Jimbei, P.; Krawczyk, A.; et al. Modelling hepatitis D virus RNA and HBsAg dynamics during nucleic acid polymer monotherapy suggest rapid turnover of HBsAg. *Sci. Rep.* **2020**, *10*, 7837. [[CrossRef](#)]
15. Koh, C.; Canini, L.; Dahari, H.; Zhao, X.; Uprichard, S.L.; Haynes-Williams, V.; Winters, M.A.; Subramanya, G.; Cooper, S.L.; Pinto, P.; et al. Oral prenylation inhibition with lonafarnib in chronic hepatitis D infection: A proof-of-concept randomised, double-blind, placebo-controlled phase 2A trial. *Lancet Infect. Dis.* **2015**, *15*, 1167–1174. [[CrossRef](#)]
16. Kadelka, S.; Dahari, H.; Ciupe, S.M. Understanding the antiviral effects of RNAi-based therapy in HBeAg-positive chronic hepatitis B infection. *Sci. Rep.* **2021**, *11*, 200. [[CrossRef](#)] [[PubMed](#)]
17. Reinharz, V.; Ishida, Y.; Tsuge, M.; Durso-Cain, K.; Chung, T.L.; Tateno, C.; Perelson, A.S.; Uprichard, S.L.; Chayama, K.; Dahari, H. Understanding Hepatitis B Virus Dynamics and the Antiviral Effect of Interferon Alpha Treatment in Humanized Chimeric Mice. *J. Virol.* **2021**, *95*, e0049220. [[CrossRef](#)] [[PubMed](#)]
18. Shirvani-Dastgerdi, E.; Tacke, F. Molecular interactions between hepatitis B virus and delta virus. *World J. Virol.* **2015**, *4*, 36–41. [[CrossRef](#)] [[PubMed](#)]
19. De Sousa, B.C.; Cunha, C. Development of mathematical models for the analysis of hepatitis delta virus viral dynamics. *PLoS ONE* **2010**, *5*, e12512. [[CrossRef](#)] [[PubMed](#)]
20. Packer, A.; Forde, J.; Hews, S.; Kuang, Y. Mathematical models of the interrelated dynamics of hepatitis D and B. *Math. Biosci.* **2014**, *247*, 38–46. [[CrossRef](#)]
21. Goyal, A.; Murray, J.M. Dynamics of in vivo hepatitis D virus infection. *J. Theor. Biol.* **2016**, *398*, 9–19. [[CrossRef](#)] [[PubMed](#)]